Optimization of conductor geometries of small RF loop coils for ultra high field applications

D. O. Brunner[1], C. Grassberger[2], and K. P. Pruessmann[1]
[1]Institute for Biomedical Engineering, University and ETH Zurich, Zurich, Zurich, Switzerland, [2]Institute for Biomedical Engineering, University and ETH Zurich, Zurich, Switzerland

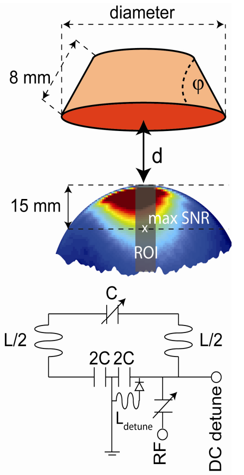

Figure 1: *Geometry of the setup used for comparison (top), schematic of the coil tuning matching and detuning (bottom).*

Introduction: Receive-only loop coils and arrays thereof are common practice for surface detection in MRI. Recently it has been shown that the SNR performance of such coils at high field can be increased by using cylindrical conductors rather than wire or planar conductor structures [1]. Such extended conductors allow the current distribution to vary with different loading situations reducing the over all series resistance introduced by the sample load. This allows the current to evade high resistances introduced by proximity effects and localized capacitive coupling to the sample. The goal of this work was to experimentally explore geometrical variations of such conductor shapes for the application in human ultra high field systems (7T) in order to improve the coupling efficiency to the sample.

Methods: Figure 1 shows the basic coil geometry that has been considered. 8-mm-wide adhesive copper tape was mounted around truncated-cone PMMA formers with a diameter of 30 mm facing the sample. The angle of the shell was varied between 90 and -45 degree, where negative angles indicate tapering of the cone towards the sample. A cylindrical shape was thus characterized by 90°. Considering each circumferential current path as a separate parallel circuit, it was expected, that conical coils act similarly like a collection of coils with different diameters in different distances. Thereby the tilting angle of the cone should allow optimizing the SNR profile of the coil. The penetration depth as a function of coil size was explored by building coils with diameters of 25 and 45 mm for comparison. The total inductance as well as unloaded and loaded Q factors were measured using a network analyzer (Tab. 1).

The signal-to-noise ratio (SNR) was averaged from images over ROIs of (10 x 10) mm^2 at varying depths. Due to the asymmetry of B_1 at high Larmor frequencies the profiles were taken with a lateral shift which was determined by the maximum SNR in 15 mm depth. . Three phantoms were made by filling polyethylene bottles of 100 mm in diameter with mineral oil (Marcol 82, ε=2.3, σ~0), tissue-simulating liquid (ε=58, σ=0.78 $^S/_m$), and tissue-conductive copper-sulfate-doped saline water (ε=80, σ=8 $S/_m$), respectively. The coils were placed with a spacing d of 3 mm and 8 mm from the surface. The 45/30 coil was also used to image a kiwi fruit with very high in-plane resolution of 50 µm at a slice thickness of 1.5 mm (3D gradient-echo sequence, 4 slices, 15 min). In-vivo images were obtained from a human wrist with a maximum resolution of 120 µm in-plane at a slice thickness of 2 mm (T_1 enhanced gradient echo, 10 slices, 10 min).

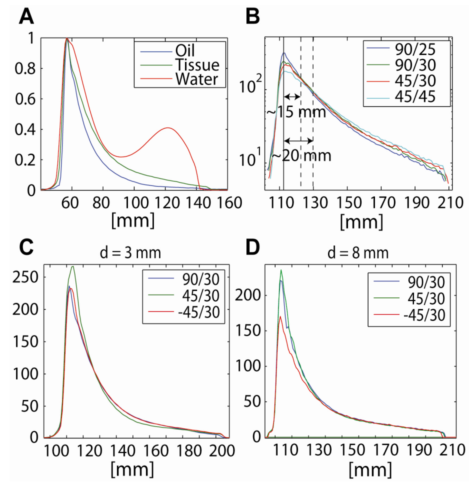

Figure 2: *SNR vs. penetration depth for coil 0/30 for different dielectric properties (A), different coil diameters (B), different coil geometries 3 mm (C) and 8 mm distant from the tissue dielectric sample (D).*

Name	φ [°]	∅ [mm]	L [nH]	Q unl.	Q load	Q drop
90/25	0	25	37	140	62	2.3
90/30	0	30	47	240	57	4.2
45/30	90	30	39	210	40	5.3
-45/30	-90	30	54	165	69	2.4
45/45	90	45	84	210	25	8.4

Table 1: *Coil parameters*

Results & Discussion: It has been seen that the Q drop for the 25 mm coil is about 2.3 meaning that the coil losses and the sample losses are about equal. This suggests a lower boundary for the size of coil elements in large receiver arrays at these frequencies. The penetration depth (e.g. for coil 90/30 in Fig.1A) is vastly dependent on the sample. Even in these relatively small phantoms, the dielectric effects are more prominent than the sensitivity decay due to the loss-induced skin effect in the conductive sample. Hence the penetration depth increases with the dielectric permittivity of the sample and is even higher than in the lossless case using an oil phantom. In the case of a water phantom, the coil sensitivity exhibits even a second maximum at the opposite side of the phantom. Using the tissue dielectric phantom it is shown that starting from a penetration of about the radius of the coil the SNR is higher than with a smaller coil which is marked by the dashed lines in Fig. 1B for the pairs of coils 90/25 vs. 90/30 and 45/30 vs. 45/45.

Conclusion: The SNR profiles in Fig. 2 C&D suggest that an angulation of 45° results in a higher SNR close to the surface especially for close placements of the coil. Although the SNR profile is steeper than for a cylindrical coil, the angulation is advantageous up to a penetration depth of 30 mm at which a bigger coil outperforms any of these geometries anyways. It has been found by comparing coils with different diameters (Fig.2B) that for dielectrically dominated samples, e.g. as tissue, the optimal radius of a coil for a targeted penetration depth is reasonably bigger than reported for lower frequencies [2] because the dielectric effects reduce the concentration of the field close to the coil (Fig.1A). Even on these rather small phantoms the electromagnetic properties of the sample material and its geometry have a more dominant impact than the conductor geometry. For electrically big objects the advantage of high local SNR close to a single coil is thereby seriously reduced which makes the use of single small coil unfavorable. However on smaller objects the conical coil 45/30 allowed high resolution imaging of small structures such as cartilage in the wrist or a kiwi fruit (Fig.3).

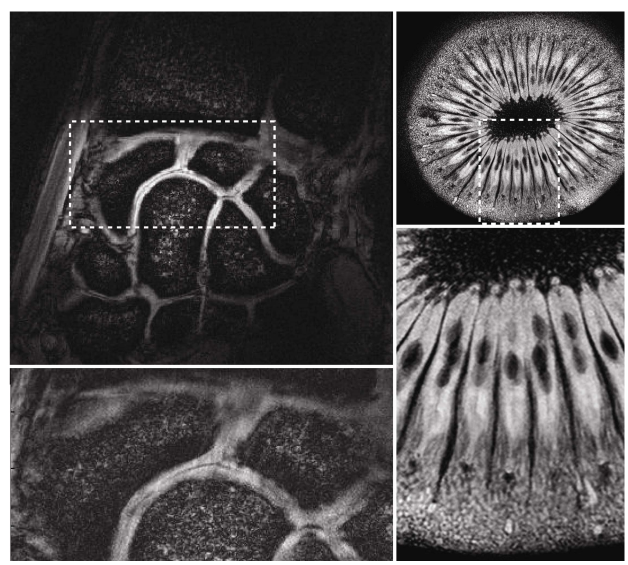

Figure 3: *Left: human wrist in vivo, resolution = 120 µm in-plane. Right: kiwi fruit, resolution = 50 µm in-plane.in/8 slices).*

References: [1] G. C. Nascimento ISMRM 2008 p.442 [2] S.B. King et al. MRM 1999